Depletion Effects Massively Change Chromatin Properties and Influence Genome Folding

Philipp M. Diesinger[†*] and Dieter W. Heermann[†‡§]
[†]Institut für Theoretische Physik and [‡]Interdisziplinäres Zentrum für Wissenschaftliches Rechnen, Heidelberg University, Heidelberg, Germany; and [§]Institute for Molecular Biophysics, The Jackson Laboratory, Bar Harbor, Maine

ABSTRACT We present a Monte Carlo model for genome folding at the 30-nm scale with focus on linker-histone and nucleosome depletion effects. We find that parameter distributions from experimental data do not lead to one specific chromatin fiber structure, but instead to a distribution of structures in the chromatin phase diagram. Depletion of linker histones and nucleosomes affects, massively, the flexibility and the extension of chromatin fibers. Increasing the amount of nucleosome skips (i.e., nucleosome depletion) can lead either to a collapse or to a swelling of chromatin fibers. These opposing effects are discussed and we show that depletion effects may even contribute to chromatin compaction. Furthermore, we find that predictions from experimental data for the average nucleosome skip rate lie exactly in the regime of maximum chromatin compaction. Finally, we determine the pair distribution function of chromatin. This function reflects the structure of the fiber, and its Fourier-transform can be measured experimentally. Our calculations show that even in the case of fibers with depletion effects, the main dominant peaks (characterizing the structure and the length scales) can still be identified.

INTRODUCTION

Nucleosomes are the basic repeat unit of chromatin fibers (1,2) in all eukaryotic organisms. They consist of a central histone octamer and a stretch of DNA ($\approx$150 basepairs (bp)), which is wrapped around the histone complex. The histone octamer consists of four pairs of core histones (H2A, H2B, H3, and H4) and is known up to atomistic resolution (3,4). Nucleosomes are connected by naked DNA strands of ~50-bp length, and together with these linkers they form the so-called chromatin fiber.

The histone H1 (and the variant histone H5 with similar structure and functions) is involved in the packing of the beads on a string structure into the 30-nm chromatin structure. It keeps in place the in- and outgoing DNA strand by binding the two of them at the same time and thus stabilizes the nucleosome. H1 depletion can cause dramatic alterations in the chromatin structure (5). The nucleosome provides the first level of compaction and, furthermore, it is important in the regulation of transcription. Several enzymes can change the position of the nucleosome (6) along the DNA.

The chromatin fiber's degree of compaction depends on the salt concentration (7) and on the presence of linker histones (8). In vitro experiments show that, at low salt concentration, a 10-nm structure is formed that has the shape of beads on a string (7), whereas at high salt concentrations the chromatin fiber is much more compact and has a diameter of ~30 nm (9).

The chromatin structure is still under discussion (2,10–12). There are several different structural models: zigzag ribbon models (8,13–16), helical solenoid models (7,17,18), or those simply having no regular structure (11). A crystal structure of a tetranucleosome has been revealed (13) and used to construct a model for the 30-nm fiber, which resembles a zigzag ribbon that twists or supercoils. The chromatin fiber has been investigated by electron cryo-microscopy (8,19), atomic force microscopy (20,21), neutron scattering, and scanning transmission electron microscopy (22). Beyond the 30-nm level, chromatin is poorly understood.

Recent studies (23) showed that linker histones are not necessary for the formation of the 30-nm fiber, although they contribute to its compaction. The chromatin compaction depends not only on the presence of histone H1 and the salt concentration but on the nucleosome repeat length (NRL) (24) as well (i.e., the length of the DNA stretch that is wrapped around a nucleosome plus the length of the linker DNA that connects two consecutive nucleosomes). Routh et al. (23) showed that only the 197-bp NRL can form a 30-nm higher-order chromatin structure and that it shows a cooperative linker-histone-dependent compaction. Chromatin strands with a repeat length of 167 bp display a limited linker-histone-dependent compaction, which leads to a topologically different thinner fiber.

Widom (24) presented a large amount of measurements on NRLs in a former work. They found that the NRL distributions show preferential quantization to a set of values related by integral multiples of the helical twist of DNA. This implies that the nucleosomal DNA content ω as well as the linker DNA lengths b are preferentially quantized. Furthermore, they presented a probability distribution for the different NRLs (24).

The DNA content of a nucleosome is 147 bp. Its DNA is sharply bent and tightly wrapped around the histone protein octamer (25). This bending occurs at every DNA helical repeat (i.e., $\approx$10 bp), when the major DNA groove faces toward the histone octamer, and again $\approx$5 bp away, when the major groove faces outwards. Specific dinucleotides

Submitted March 9, 2009, and accepted for publication June 5, 2009.

*Correspondence: p.m.diesinger@gmx.de

Editor: Jonathan B. Chaires.

0006-3495/09/10/2146/8 $2.00

doi: 10.1016/j.bpj.2009.06.057

facilitate the bends of each direction (26,27). The linker DNA that connects consecutive nucleosomes has a length of ~50 bp. Thus, ~75% of genomic DNA is wrapped in nucleosomes if the chromatin fiber is entirely saturated with them. Access to DNA wrapped in a nucleosome is occluded (25) for polymerase, regulatory, repair, and recombination complexes, yet nucleosomes also recruit other proteins through interactions with their histone tail domains (28). Thus, the detailed locations of nucleosomes along the DNA may have important inhibitory or facilitatory roles in regulating gene expression (29,30).

Since DNA sequences differ in their ability to bend sharply (26,27,31), the ability of the histone octamer to wrap different DNA sequences into nucleosomes is highly dependent on the DNA sequence (32,33). In vitro studies show this range of affinities to be 1000-fold or greater (34). Thus, nucleosomes have substantial DNA sequence preferences, which results in a nonregular arrangement of the nucleosomes along the DNA. Furthermore, nucleosomes can dissolve entirely by unwrapping the DNA, leaving naked DNA stretches behind, and later on, they can reassemble. Thus, nucleosomes are in a dynamic equilibrium with the chromatin fiber. These effects lead to an average nucleosome occupation (i.e., the probability that a bp is covered by a nucleosome) of $<75\%$. Since the DNA around the histone octamer has a length of ~150 bp and the linkers have a length of 50 bp, an average nucleosome occupancy of $\approx 75\%$ corresponds to a perfect chromatin fiber where every nucleosome position is occupied.

In Segal et al. (35), in 2006, the average nucleosome occupancy was partially determined experimentally and predicted by a probabilistic model. In 2008, Segal et al. (1) had extended their model to make a prediction for the entire yeast genome, and found an average nucleosome occupancy of 68%; i.e., not all nucleosome locations are actually occupied by a histone octamer. Instead, one gets strong depletion effects that affect the chromatin fiber properties massively, as we will show below.

In this work, we present an improved chromatin model that takes nucleosome depletion as well as linker-histone depletion into account. We investigate their impact on the chromatin compaction and on the flexibility of the chromatin fiber, and show that depletion effects may even contribute to chromatin compaction.

We use the experimental data from Widom (24) to include local fluctuations in our model since the nucleosome-nucleosome interactions are still unknown. Furthermore, we use the prediction of the average nucleosome occupancy of Segal et al. (1) from 2008 as a reference value and find that it lies just in the regime of optimal chromatin compaction.

METHODS

In a previous work (36), we presented a chromatin model (E2A model) that included the possibility to study linker-histone depletion. Our algorithm avoids any potentials (except excluded volume potentials) and dynamics to keep the code fast. Thus, large equilibrated chromatin fiber conformations up to some Mbps (i.e., $\approx$10,000 NRL) can be generated. The details of this model, including a comprehensive description of the linker-histone depletion modeling that was used for this work as well, can be found in Diesinger and Heermann (36).

We improved this Monte Carlo (37) model by two significant chromatin features—those of flexibility and nucleosome depletion, which are supplied by local fiber fluctuations.

The chromatin fibers in the previous model were stiff, i.e., there were no distributions for the local fiber parameters due to the still rarely known nucleosome-nucleosome interaction potential. In a sense, the previous model was a mean-field approach to the chromatin fiber on small length scales. The nucleosome-nucleosome as well as the nucleosome-DNA interaction are highly complex and still an area of ongoing research. We solved the problem of avoiding these potentials by using experimental data (24) for the distribution of the NRL, and taking advantage of the fact that the local chromatin parameters are not independent. For this case, it is possible to partially invert the convolution of the probability distributions (which is given by the experimental data), and thus, get information on the individual distributions of our model parameters.

Making use of given parameter distributions for the model parameters gives us the advantage of saving computation time that would otherwise be spent for the equilibration of the fibers. The saved computation time can then be used to generate very large fibers (i.e., chromatin fibers consisting of several Mbp).

Of course excluded volume potentials for the DNA and the nucleosomes are still taken into account: The DNA has a tubelike shape and the nucleosomes have the excluded volume of flat cylinders.

Parameter distributions of the E2A model

In this section we show how the experimental data for the NRL distribution (24) can be used to get information about the parameter distributions of our model.

The NRL consists of a stretch of linker DNA b and the DNA content, which is wrapped around the nucleosomes ω: NRL $= b + \omega$. We use only the 197-bp repeat length peak of the data in Widom (24).

In our model, b_i is the linker length between two consecutive nucleosomes (i–1 and i) and ω_i is the length of the DNA strand covering nucleosome i.

We approximate the distribution for the nucleosome repeat length in Widom (24) by a Gaussian standard normal distribution:

$$f_{\mathrm{NRL}}(l) = \mathcal{N}[\mu_{\mathrm{NRL}}, \sigma^2_{\mathrm{NRL}}](l) = \frac{1}{\sigma_{\mathrm{NRL}}\sqrt{2\pi}}\, e^{-\frac{1}{2}\left(\frac{l-\mu_{\mathrm{NRL}}}{\sigma_{\mathrm{NRL}}}\right)^2}. \quad (1)$$

Furthermore, we know NRL $= b + \omega$, where NRL, b, and ω are random variables. Therefore, the convolution of the probability density functions of b and ω must be the probability density of NRL, i.e.:

$$f_{\mathrm{NRL}}(l) = \int_{-\infty}^{\infty} f_{\mathrm{b}}\left(l'\right) f_{\omega}\left(l - l'\right) dl'.$$

By assuming Gaussian standard normal distributions and statistical independence

$$f_{\mathrm{b}} = \mathcal{N}[b_0, \sigma^2_{\mathrm{b}}]$$
$$f_{\omega} = \mathcal{N}[\mu_{\omega}, \sigma^2_{\omega}],$$

which gives

$$\mu_{\mathrm{NRL}} = b_0 = \mu_{\omega} \text{ and } \sigma^2_{\mathrm{b}} + \sigma^2_{\omega}.$$

In this context, σ^2_{ω} represents a part of the mobility of the nucleosomes inside the DNA loops. We choose σ^2_{b} and σ^2_{ω}, proportional to the DNA

TABLE 1 Parameters of the E2A model

μ_{NRL}	197 bp	σ^2_{NRL}	1.5 bp^2
b_0	146 bp	σ^2_{b}	0.4 bp^2
β_0	36 deg	σ^2_{β}	0.1518
μ_{ω}	146 bp	ε^2_{ω}	1.1 bp^2
μ_{h}	8.4 bp	σ^2_{h}	0.0036

content of their corresponding nucleosome repeat unit parts (compare to Table 1).

The rotational angle β_{i} is a periodic function of the linker length b_{i} because DNA adsorption always begins with the minor groove turned in toward the first histone-binding site:

$$\beta(b) = \beta_0 + \frac{2\pi}{10.2\ \mathrm{bp}}(b - b_0).$$

The period is the repeat length of the helical twist of the DNA. It is fixed to 10.2 bp in this work. β_0 and b_0 are the mean values of β and b. They can be found in Table 1. With the equation above, one can calculate the probability density function of β by transforming the density of b:

$$\begin{aligned} f_{\beta}\left(\beta'\right) &= f_{\mathrm{b}}\left(b'\right)\frac{db\left(\beta'\right)}{d\beta} \\ &= \mathcal{N}[b_0, \sigma^2_{\mathrm{b}}]\left(b'\right)\left(\frac{10.2\mathrm{bp}}{2\pi}\right) \\ &= \frac{10.2\ \mathrm{bp}}{2\pi}\frac{1}{\sigma_{\mathrm{b}}\sqrt{2\pi}}\exp\left[-\frac{1}{2}\left(\frac{b_0 + 10.2\ \mathrm{bp}\left(\frac{\beta' - \beta_0}{2\pi}\right) - b_0}{\sigma_{\mathrm{b}}}\right)^2\right] \\ &= \mathcal{N}\left[\beta_0, \left(\frac{2\pi}{10.2\ \mathrm{bp}}\sigma_{\mathrm{b}}\right)^2\right]\left(\beta'\right). \end{aligned}$$

In our model, β_{i} depends directly on b_{i}. Its distribution was calculated here for the sake of completeness.

Similarly, one can calculate the density function of h by the relation

$$h = \frac{1}{2}\left(\frac{8.4\ \mathrm{bp}}{146\ \mathrm{bp}}\omega_{\mathrm{i}-1} + \frac{8.4\ \mathrm{bp}}{146\ \mathrm{bp}}\omega_{\mathrm{i}}\right) = \frac{8.4}{292}(\omega_{\mathrm{i}-1} + \omega_{\mathrm{i}}).$$

Here, $\omega_{\mathrm{i}-1}$ and ω_{i} are statistically independent random variables with the same probability density f_{ω}. Therefore, one gets the probability density of h by

$$\begin{aligned} f_{\mathrm{h}}\left(h'\right) &= f_{\omega_{\mathrm{i}-1}+\omega_{\mathrm{i}}}\left(\omega'\right)\frac{292}{8.4} \\ &= \mathcal{N}\left[2\mu_{\omega}, (2\sigma_{\omega})^2\right]\left(\frac{292}{8.4}h'\right)\frac{292}{8.4} \\ &= \mathcal{N}\left[\frac{8.4}{292}2\mu_{\omega}, \left(\frac{8.4}{292}2\sigma_{\omega}\right)^2\right]\left(h'\right). \end{aligned}$$

The results for the parameter distributions in our model are shown in Fig. 1 and in Table 1. An example conformation with these parameter distributions is illustrated in Fig. 2 *b*. With these parameter distributions, the E2A model complies with the scaling laws for a self-avoiding walk at very large length scales. For smaller scales (up to ≈5000 NRLs), the end-to-end distance and the radius of gyration show strong finite size effects.

Nucleosome depletion

The second chromatin feature that we included in the model is the possibility for nucleosomes to dissolve entirely so that only naked DNA stretches remain. These DNA strands are modeled as wormlike chains with a diameter

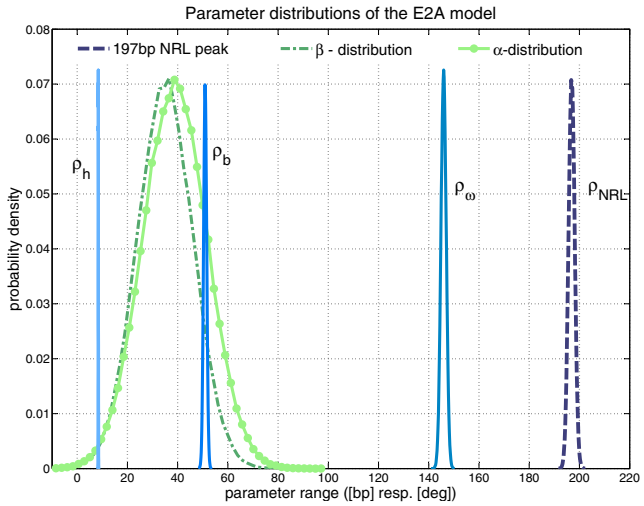

FIGURE 1 This figure shows the underlying parameter distributions of our model. They are obtained from the NRL distribution of Widom (24) and are used instead of interaction potentials since these, in analytical form, are not known to date.

of 2.2 nm and a persistence length of 50 nm as illustrated in Fig. 3 *a*. In a real-cell nucleus, nucleosome-free regions are likely to be occupied by regulatory proteins.

To estimate the average rate of nucleosome skips, we used data for the average nucleosome occupancy per bp (35) that was obtained by experiments combined with a probabilistic prediction model. We use a prediction of the nucleosome occupancy for the entire yeast genome (1).

The transformation between the average nucleosome occupancy n in the literature (1,35) and the nucleosome skip probability p_{nuc} in this model is

$$p_{\mathrm{nuc}} = 1 - n\frac{197\ \mathrm{bp}}{147\ \mathrm{bp}} = 1 - 1.34n.$$

With a linker length of ~50 bp and ≈150 bp wrapped around each histone complex, one would expect an average nucleosome occupancy of ≈75% for a perfectly regular chromatin strand—i.e., a nucleosome occupancy of $n \approx 75\%$ leads to a vanishing skip rate. On the other hand, if $n = 0$, i.e., there were no nucleosomes at all, the nucleosome skip rate p will be 100%. A negative value for the nucleosome skip probability means that even more base-pairs are covered by nucleosomes than expected by a regular, ideal chromatin strand. In this case, the linker lengths between the nucleosomes have to be adjusted (i.e., narrowed) to get the given nucleosome occupancy n.

The predicted nucleosome occupancy for the yeast genome (1) has a mean value of ≈68%, which means that one should expect a nucleosome skip rate of 8% for an average chromatin fiber. The yeast (*Saccharomyces cerevisiae*) genome is special in some ways since it has a very high gene density and essentially no heterochromatin. Probably the genomes of most other eukaryotes have lower nucleosome skip rates. Therefore, the nucleosome skip rate will be treated as a variable parameter in the following section.

Two conformations for chromatin fibers with a nucleosome skip rate of 8% and an estimated linker-histone skip rate of 6% are shown in Fig. 3 *b* and Fig. S1 in the Supporting Material. Later on, the skip rates are treated as parameters in our model, i.e., they are varied over a large range of possible values to see how depletion effects affect chromatin properties.

In this work, linker-histone depletion and nucleosome depletion are treated statistically independently, to investigate the two different kinds of chromatin defects separately from each other. In fact, linker-histone depletion facilitates nucleosome depletion, because if the glue particle that keeps the in- and outgoing DNA strand together is missing, it is much easier for the DNA to unroll from the histone octamer. The linker histone corresponds to an energy barrier that inhibits the unrolling of the DNA arms.

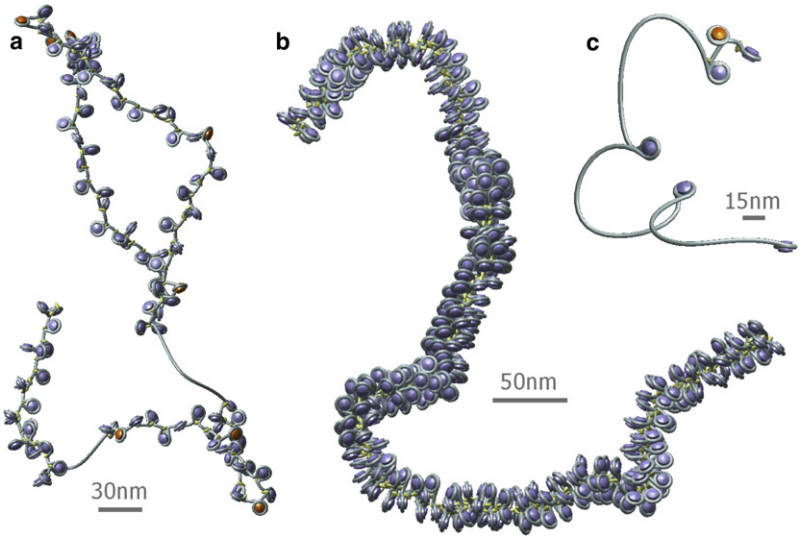

FIGURE 2 Examples of conformations generated within the framework of the model if one takes the empirical parameter distributions as well as the depletion effects into account. Similar electron micrographs can be found in Olins and Olins (40). (*a*) Shows a beads-on-a-string-like structure with some nucleosome and linker-histone skips. The latter are marked orange. (*b*) Example conformation of a chromatin strand of length 40 kbp. The light blue tubes represent the DNA, the histone octamers are modeled as purple cylinders, and the linker histones are marked in light yellow. This chromatin conformation has no depletion effects and a diameter of ~34 nm. (*c*) One can even get single nucleosomes connected by naked DNA stretches, which is shown here.

RESULTS

Comparing Fig. 2 *b* (i.e., a chromatin fiber without nucleosome or linker-histone depletion) with fiber conformations that allow for depletion effects (Fig. 3 *b* and Fig. S1), one can easily see that an expectation of a regular 30-nm chromatin fiber is no longer justified. Instead, one gets a coil-like structure of some more or less regular parts separated by very flexible parts, which mainly consist of naked DNA stretches. The linker-histone depletion does not destroy the picture of a regular 30-nm fiber as much as the nucleosome depletion. Moreover, one has to keep in mind that the nucleosome depletion rate which was used to generate the conformations in Fig. 3 *b* and Fig. S1) is only the average depletion rate (of the yeast genome). Some parts of the genome (for instance, telomeres (1,35)) have even larger nucleosome depletion rates, and therefore are much more coiled. Furthermore, small nucleosome skip rates already induce very coiled structures. The crossed-linker parts of the chromatin fibers generated with our model had an average radius of 34.6 nm and a nucleosome line density of 5.8 nucleosomes per 11 nm. Their persistence length was $\approx$280 nm.

A comprehensive discussion of the phase diagram for regular (i.e., stiff) chromatin fibers can be found in the literature (15,38,36,39).

The parameter distributions lead to fibers that no longer have a fixed structure (or topology). Instead, one gets a probability distribution of structures (shown in the *background* of Fig. 4). One can see that the main part of the chromatin fiber is still a crossed-linker fiber, but some smaller parts can be in a more open beads-on-a-string-like state or another state. (Some examples are shown in Fig. 2.) A visual comparison with electron micrographs (40) shows strong similarities.

Fig. 5 shows how either linker-histone or nucleosome depletion affects the flexibility of chromatin fibers. Without any depletion effects (i.e., zero skip rate), the fiber has a persistence length of ~280 nm. If the skip rate for either linker histones or nucleosomes increases, the persistence length drops very fast in both cases, i.e., the fiber gets much more flexible. Fig. 6 shows the persistence length as

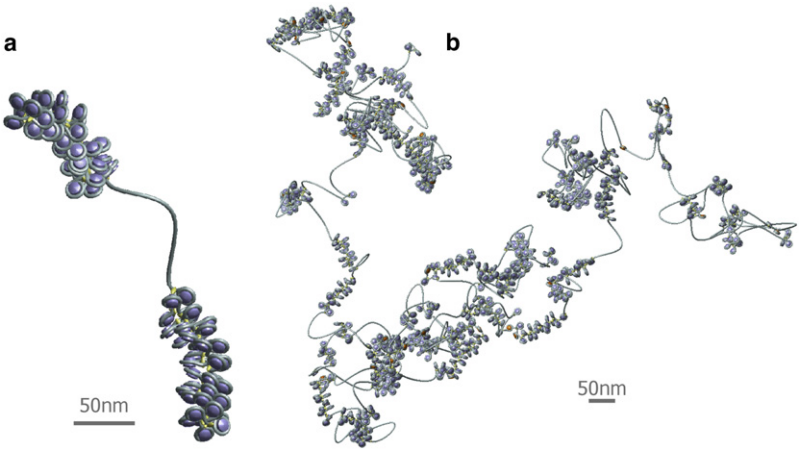

FIGURE 3 (*a*) Example of a single nucleosome skip. If a nucleosome is dissolved, a blank stretch of DNA remains. The naked DNA stretches have lengths of multiple integers of the nucleosome repeat length plus once the length of a DNA linker, and can lead either to a collapse or to a swelling of the chromatin fiber. In both cases, they increase the flexibility of the chromatin chain massively. (*b*) Example conformation of a chromatin fiber with depletion effects: The linker -histone skip rate is 6% and the nucleosome skip rate is 8%. The linker-histone skips are marked orange. One can see that the concept of a regular 30-nm fiber no longer holds. Instead, one obtains very flexible coil-like structures of compact regions that are separated by naked DNA stretches. The fiber has a total length of 394 kbp.

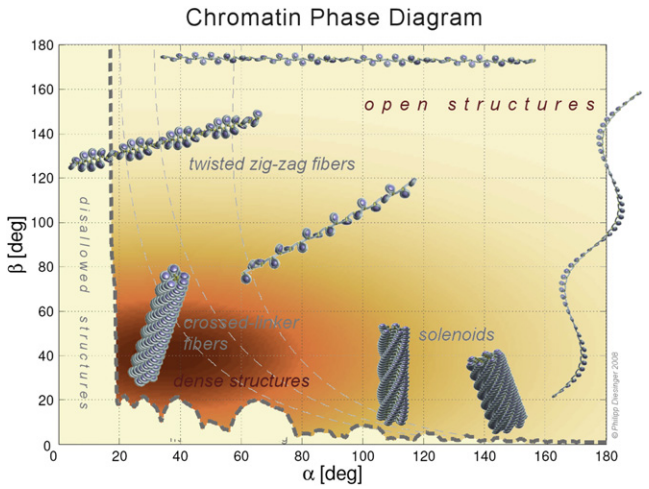

FIGURE 4 Cutout of the actual four-dimensional chromatin phase diagram. The pitch d and the linker length b are fixed here. A single point in this diagram corresponds to a specific chromatin structure. The forbidden structures lie left and below the dashed line, which is the excluded volume borderline (38). Due to the parameter distributions in our model, we do not expect a specific chromatin structure but instead a distribution of structures in the phase diagram. This probability distribution is shown in the back of the figure.

a function of the skip rates, but this time, combinations of the two kinds of depletion effects are considered as well.

We used the radius of gyration as well as the mean-squared end-to-end distance as a measure for the fiber extension to see how it is changed by the depletion effects. In Fig. S2 and Fig. 7, one can see how either linker-histone depletion or nucleosome depletion affect the fiber extension, and Fig. S3 and Fig. 8 again show the same results for the combination of the two depletion effects.

In the case of linker-histone skips, the fiber extension decreases with increasing skip rate, until it reaches a skip

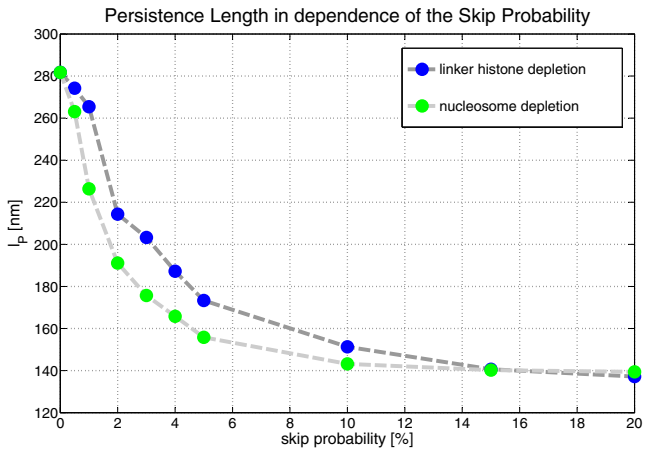

FIGURE 5 This figure shows how depletion effects decrease the chromatin persistence length l_P. Here, either linker-histone or nucleosome depletion effects are considered. The persistence length decreases very similarly for both cases. Nucleosome depletion has a slightly larger effect for small skip rates.

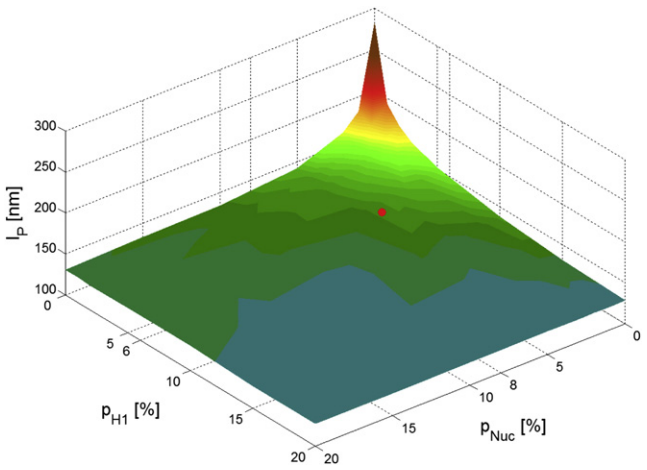

FIGURE 6 This figure shows how depletion effects decrease the chromatin persistence length l_P. In this case, combinations of linker-histone and nucleosome depletion effects are considered. The red spot marks the expected average rates for the two depletion effects.

rate of $\approx 15\%$. In terms of chromatin compaction, this means it could even be necessary to have a linker-histone depletion of ~15% or vice versa: It is not efficient to have >85% of all nucleosomes saturated with H1 histones, because at some point the fiber gets too stiff, and therefore, no longer bends so easily.

Increasing the nucleosome skip rate has two effects on the chromatin fiber: First, it gets more flexible, due to the naked DNA stretches that connect regions that are more compact.

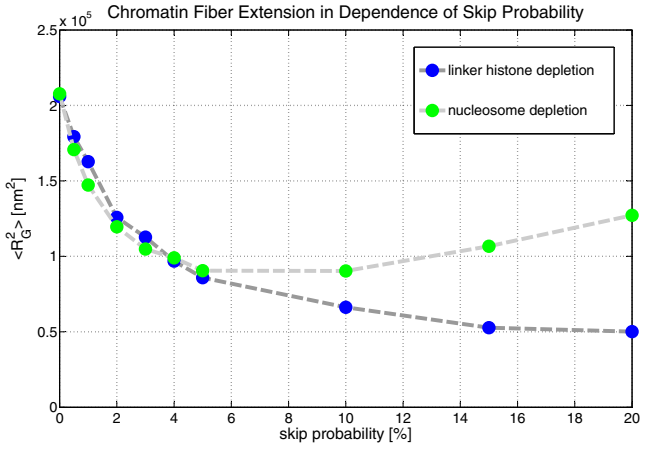

FIGURE 7 Mean-squared radius of gyration is used as a measure for the extension of the chromatin fiber. With increasing linker-histone depletion (*blue*) it decreases, whereas with increasing nucleosome depletion (*green*) there is a plateau regime after a initial decrease and at the end, the fiber extension even increases. These effects come, on the one hand, from the gain of flexibility that the nucleosome skips bring in, and on the other hand, from the spatial need of naked DNA, in opposite to the compact wrapped DNA. In the plateau regime, these two effects level off. This is the regime where chromatin compaction is optimal. As one can see, the experimental values for the nucleosome skip-rate with an average of 8% lie just in this region of optimal condensation.

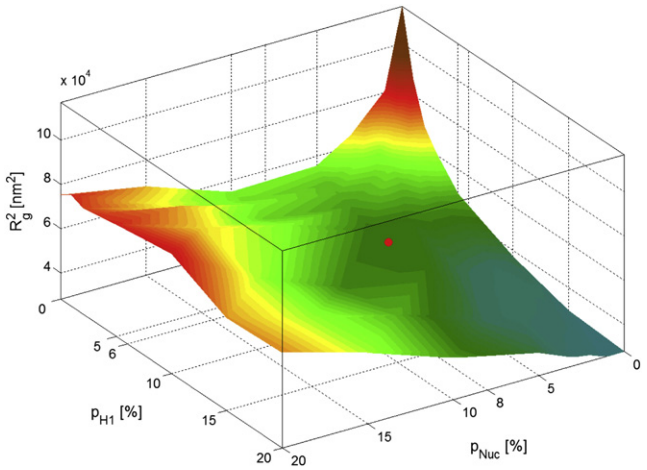

FIGURE 8 Mean-squared radius of gyration as a measure of the extension of the chromatin fibers in the dependence of depletion effects. Here, again, are combinations of linker-histone and nucleosome depletion effects possible. The red spot marks again the expected average values that come from experimental data.

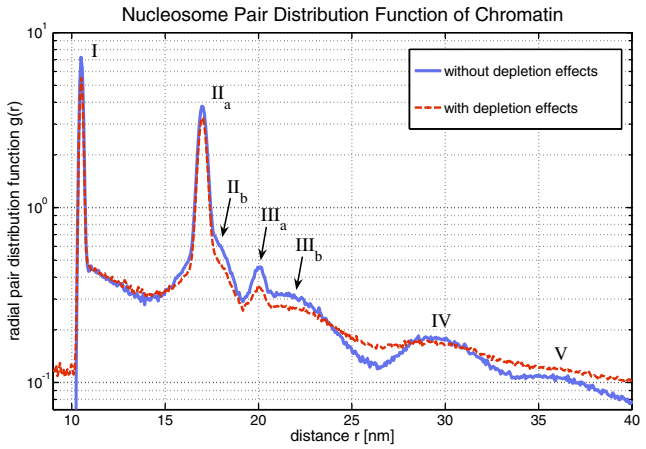

FIGURE 9 Pair-distribution function of nucleosomes in a chromatin fiber (with and without depletion effects). The value $g(r)$ is proportional to the probability of finding a nucleosome in distance r to a reference nucleosome. The labeled peaks can be associated with particular genomic nucleosome-nucleosome distances Δ (compare to Table 2). Even in the case of fibers with depletion effects (i.e., a linker-histone skip rate of 6% and a nucleosome skip rate of 8%), the first four peaks can be clearly identified.

Second, the naked DNA is much less condensed, and thus, needs more space due to entropic forces than the DNA, which is wrapped up around histone octamers. In Fig. 7 and Fig. S2, one can see that the fiber extension first decreases with increasing nucleosome depletion (0–5%), then there is a plateau regime where it is almost constant (5–9%) and finally it increases again (>9%). The first decrease comes from the increase of flexibility, which the naked DNA stretches bring in. The increase of the extension at the end (>9%) stems from the spatial need of the naked DNA, and in the plateau regime at the middle, the two effects level off.

One can also consider this from the view of chromatin compaction: At a nucleosome skip rate of 100%, one would have the whole genome as a naked stretch of DNA. Adding nucleosomes means that one decreases the nucleosome skip rate now. At the plateau regime, the chromatin compaction is optimal because a further increase makes the chromatin fiber too stiff. One has to keep in mind that the experimental data for the average nucleosome occupancy (1) suggested an average nucleosome skip rate of 8%, which lies just in this plateau regime of optimal chromatin compaction. This means the experimentally determined average nucleosome occupancy is optimal in terms of chromatin compaction.

Fig. 9 shows the (radial) pair distribution function $g(r)$ (41) of nucleosomes in a chromatin strand. The pair distribution function is a major descriptor for the atomic structure of solids, amorphic materials, and liquids. In this case, we can apply this mathematical tool only for small distances, because we do not have a chromatin melt but instead, only a single fiber at a time. Therefore, the distance cutoff for the following structure analysis was set to a small value, namely 40 nm. Hence, we analyze spheres with this radius around each nucleosome by looking for very frequent spatial distances. In this context it is important to keep in mind that the nucleosomes sit at the edge of the chromatin fiber and furthermore, the fiber has only a diameter of ~35 nm. Therefore, the main part of the 40-nm-sphere is empty, which leads to a decrease of the mean nucleosome density (compare to Fig. 9).

The pair-distribution function is proportional to the conditional probability of finding a nucleosome at a distance r if another nucleosome is sitting at the origin. It is normalized so that a value of one corresponds to the mean nucleosome density of the considered system (i.e., in this case a 40-nm sphere). The pair correlation function is given by $g(r)$–1 and the Fourier-transform of it is the scattering function $S(q)$, which could be determined by scattering experiments.

Fig. 9 shows some very dominant nucleosome-nucleosome distances, which are labeled I–V. These peaks, representing frequent spatial distances r_Δ, can be associated with genomic distances between nucleosomes in the chromatin fiber (compare to Table 2). These genomic distances are denoted by Δ and they are given in multiples of the nucleosome repeat lengths (i.e., they are integer numbers). The corresponding spatial nucleosome-nucleosome distance to a genomic distance Δ is denoted by r_Δ. In this sense, $g(r)$ is the superposition of all r_Δ-distributions.

Some of the peaks in Fig. 9 are superpositions of several single distributions $P(r_\Delta)$. This is indicated in some cases by subscript letters (compare to peaks II and III). The allocation of the peaks to genomic nucleosome-nucleosome

TABLE 2 Allocation of peak number to particular genomic nucleosome-nucleosome distances for the first five peaks in the pair distribution function *g(r)*

Peak number	I	IIa	IIb	IIIa	IIIb	IV	V
Genomic distance Δ [NRL]	2	1	3	4	5	6, 7	8, 9, 10

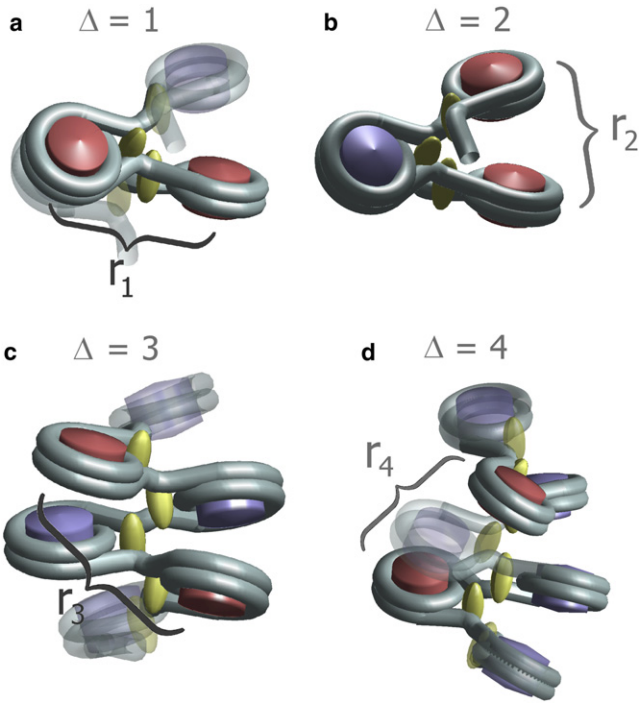

FIGURE 10 This figure illustrates the connection between the genomic distance Δ and the spatial distance r_Δ for the first four cases. The reference nucleosomes that have the genomic distance Δ (in NRLs) are marked in red.

distances can be found in Table 2. For instance, the second peak (II) is a superimposition of the distribution of r_1 and the distribution of r_3. Some of the genomic distances r_Δ are illustrated in Fig. 10. Moreover, in some cases the r_Δ-distributions are very asymmetric, which can be seen in Table S1: The mean value and the most frequent value differ greatly in some cases.

The first four peaks of the pair distribution function can even be identified if one allows for depletion effects (compare to Fig. 9), although in this case, the pair-distribution function is decreased in comparison to $g(r)$ without depletion effects because the skips reduce the number of nucleosomes that have a certain genomic distance. Nevertheless, the peaks can still be identified clearly.

DISCUSSION

Fig. 3 *b* and Fig. S1 suggest that the concept of a specific regular 30-nm chromatin fiber possibly has to be adjusted toward a distribution of structures (compare to Fig. 4), which coexist in one chromatin fiber. Furthermore depletion effects which obviously occur in vivo lead to much more coiled conformations even at small skip rates than one would expect from existing chromatin models (2,7,8,10–18,36,38). These coils surely show small stretches of 30-nm fibers that are separated by large pieces of naked DNA, but a perfectly regular 30-nm fiber seems to be very unlikely since it needs to be almost completely saturated with nucleosomes. Even from a thermodynamic point of view, this seems unlikely: Nucleosomes have the ability to dissolve and form again (for example, with the help of enzymes and proteins that are targeted to specific genomic sites by sequence-specific binding proteins), so a dynamic equilibrium resulting in a certain nucleosome skip rate seems very plausible. Perhaps these regular fibers exist only in heterochromatin-like configurations or under lab conditions, where they are built-up at high histone concentrations and therefore are entirely saturated with nucleosomes and linker histones.

Our investigation of the chromatin fiber extension in the dependence of the depletion rates shows that the nucleosome skip-rates from experimental data (1) lie in the regime of optimal chromatin compaction. This could be a hint that cells are in fact using the plateau regime to keep the DNA compact. Furthermore, cells could use the plateau regime to regulate the chromatin fiber extension locally. Transcription as well as replacement of nucleosomes by other proteins on regulatory sites may increase the nucleosome skip rate in a genome region, and thus, lead automatically to swelling of the chromatin strand. The nucleosome skips are much more important for this effect than the linker-histone skips (compare to Fig. 7 and Fig. S2).

We showed that nucleosome and linker-histone depletion may even be useful for chromatin compaction, because they give the chromatin fiber more flexibility, leading to more-compact fiber conformations (at low skip-rates). Therefore, H1 and nucleosome skips may play a very important role for chromatin compaction, and support a tool to locally regulate the chromatin-fiber extension within the cell nucleus.

SUPPORTING MATERIAL

Three figures and one table are available at http://www.biophysj.org/biophysj/supplemental/S0006-3495(09)01310-1.

We thank the Heidelberg Graduate School of Mathematical and Computational Methods for the Sciences for partial funding.

REFERENCES

1. Segal, E., et al. 2008. Average nucleosome occupancy for the whole yeast genome. http://genie.weizmann.ac.il/pubs/nucleosomes06/segal06_data.html.
2. van Holde, K. E. 1989. Chromatin. Springer-Verlag, New York.
3. Davey, C. A., D. F. Sargent, K. Luger, A. W. Maeder, and T. J. Richmond. 2002. Solvent mediated interactions in the structure of the nucleosome core particle at 1.9 Å resolution. *J. Mol. Biol.* 319:1097–1113.
4. Luger, K., A. W. Mader, R. K. Richmond, D. F. Sargent, and T. J. Richmond. 1997. Crystal structure of the nucleosome core particle at 2.8 Ångstrom resolution. *Nature.* 389:251–260.
5. Fan, Y., T. Nikitina, J. Zhao, T.S. Fleury, R. Bhattacharyya, et al. 2005. Histone H1 depletion in mammals alters global chromatin structure but causes specific changes in gene regulation. DOI:10.1016/J.Cell.2005.10.028.
6. Lia, G., E. Praly, H. Ferreira, C. Stockdale, Y. C. Tse-Dinh, et al. 2006. Direct observation of DNA distortion by the RSC complex. *Mol. Cell.* 21:417–425.

7. Thoma, F., T. Koller, and A. Klug. 1979. Involvement of histone H1 in the organization of the nucleosome and of the salt-dependent superstructures of chromatin. *J. Cell Biol.* 83:403–427.
8. Bednar, J., R. A. Horowitz, S. A. Grigoryev, L. M. Carruthers, J. C. Hansen, et al. 1998. Nucleosomes, linker DNA, and linker histone form a unique structural motif that directs the higher-order folding and compaction of chromatin. *Proc. Natl. Acad. Sci. USA.* 95:14173–14178.
9. Widom, J. 1986. Physicochemical studies of the folding of the 100 Å nucleosome filament into the 300 Å filament. *J. Mol. Biol.* 190: 411–424.
10. Chakravarthy, S., Y. J. Park, J. Chodaparambil, R. S. Edayathumangalam, and K. Luger. 2005. Structure and dynamic properties of nucleosome core particles. *FEBS Lett.* 579:895–898.
11. Van Holde, K., and J. Zlatanova. 1995. Chromatin higher order structure: chasing a mirage? *J. Biol. Chem.* 270:8373–8376.
12. Van Holde, K., and J. Zlatanova. 1996. What determines the folding of the chromatin fiber? *Proc. Natl. Acad. Sci. USA.* 93:10548–10555.
13. Schalch, T., S. Duda, D. F. Sargent, and T. J. Richmond. 2005. X-ray structure of a tetranucleosome and its implications for the chromatin fiber. *Nature.* 436:138–141.
14. Woodcock, C. L., S. A. Grigoryev, R. A. Horowitz, and N. Whitaker. 1993. A chromatin folding model that incorporates linker variability generates fibers resembling the native structures. *Proc Natl. Acad. Sci. USA.* 90:9021–9025.
15. Schiessel, H., W. M. Gelbart, and R. Bruinsma. 2001. DNA folding: structural and mechanical properties of the two-angle model for chromatin. *Biophys. J.* 80:1940–1956.
16. Dorigo, B., T. Schalch, A. Kulangara, S. Duda, R. R. Schroeder, et al. 2004. Nucleosome arrays reveal the two-start organization of the chromatin fiber. *Science.* 306:1571–1573.
17. Finch, J. T., and A. Klug. 1976. Solenoidal model for superstructure in chromatin. *Proc. Natl. Acad. Sci. USA.* 73:1897–1901.
18. Widom, J., and A. Klug. 1985. Structure of the 300 Å chromatin filament: X-ray diffraction from oriented samples. *Annu. Rev. Biophys. Chem.* 43:207–213.
19. Bednar, J., R. A. Horowitz, J. Dubochet, and C. L. Woodcock. 1995. Chromatin conformation and salt-induced compaction: three-dimensional structural information from cryoelectron microscopy. *J. Cell Biol.* 131:1365–1376.
20. Leuba, S. H., G. Yang, C. Robert, B. Samori, K. van Holde, et al. 1994. Three-dimensional structure of extended chromatin fibers as revealed by tapping-mode scanning force microscopy. *Proc. Natl. Acad. Sci. USA.* 91:11621–11625.
21. Zlatanova, J., S. H. Leuba, and K. van Holde. 1998. Chromatin structure revisited. *Biophys. J.* 74:2554–2566.
22. Gerchman, S. E., and V. Ramakrishhnan. 1978. Chromatin higher-order structure studied by neutron scattering and scanning transmission electron microscopy. *Proc. Natl. Acad. Sci. USA.* 84:7802–7806.
23. Routh, A., S. Sandin, and D. Rhodes. 2008. Nucleosome repeat length and linker histone stoichiometry determine chromatin fiber structure. *Proc. Natl. Acad. Sci. USA.* 105:8872–8877.
24. Widom, J. 1992. A relationship between the helical twist of DNA and the ordered positioning of nucleosomes in all eukaryotic cells. *Proc. Natl. Acad. Sci. USA.* 89:1095–1099.
25. Richmond, T. J., and C. A. Davey. 2003. The structure of DNA in the nucleosome core. *Nature.* 423:145–150.
26. Satchwell, S. C., H. R. Drew, and A. A. Travers. 1986. Sequence periodicities in chicken nucleosome core DNA. *J. Mol. Biol.* 191:659–675.
27. Widom, J. 2001. Role of DNA sequence in nucleosome stability and dynamics. *Q. Rev. Biophys.* 34:269–324.
28. Jenuwein, T., and C. D. Allis. 2001. Translating the histone code. *Science.* 293:1074–1080.
29. Kornberg, R. D., and Y. Lorch. 1999. Twenty-five years of the nucleosome, fundamental particle of the eukaryote chromosome. *Cell.* 98: 285–294.
30. Wyrick, J. J. 1999. Chromosomal landscape of nucleosome-dependent gene expression and silencing in yeast. *Nature.* 402:418–421.
31. Trifonov, E. N. 1980. Sequence-dependent deformational anisotropy of chromatin DNA. *Nucleic Acids Res.* 8:4041–4053.
32. Sekinger, E. A., Z. Moqtaderi, and K. Struhl. 2005. Intrinsic histone-DNA interactions and low nucleosome density are important for preferential accessibility of promoter regions in yeast. *Mol. Cell.* 18:735–748.
33. Anderson, J. D., and J. Widom. 2001. Poly(dA-dT) promoter elements increase the equilibrium accessibility of nucleosomal DNA target sites. *Mol. Cell. Biol.* 21:3830–3839.
34. Thaström, A. 1999. Sequence motifs and free energies of selected natural and non-natural nucleosome positioning DNA sequences. *J. Mol. Biol.* 288:213–229.
35. Segal, E., Y. Fondufe-Mittendorf, L. Chen, A. Thaström, Y. Field, et al. 2006. A genomic code for nucleosome positioning. *Nature.* DOI: 10.1038/nature04979.
36. Diesinger, P. M., and D. W. Heermann. 2007. The influence of the cylindrical shape of the nucleosomes and H1 defects on properties of chromatin. *Biophys. J.* 94:4165–4172.
37. Binder, K., and D. W. Heermann. 2002. The Monte Carlo Method in Statistical Physics, 4th Ed. Springer Series in Solid-State Sciences. Springer, NY
38. Diesinger, P. M., and D. W. Heermann. 2006. Two-angle model and phase diagram for chromatin. *Phys. Rev. E Stat. Nonlin. Soft Matter Phys.* 74:031904.
39. Schiessel, H. 2003. The physics of chromatin. *J. Phys. Condens. Matter.* 15:R699–R774.
40. Olins, D. E., and A. L. Olins. 2003. Chromatin history: our view from the bridge. *Nat. Rev. Mol. Cell Biol.* 4:809–814.
41. Strobl, G. 2007. The Physics of Polymers: Concepts for Understanding their Structures and Behavior, 3rd Ed. Springer, NY.